

ESTIMATION OF AIRFLOW IN LIVESTOCK BUILDINGS USING IMAGE ANALYSIS



Rasmus Larsen
Assistant (Research) Professor
Department of Mathematical Modelling
Technical University of Denmark
Building 321
DK-2800 Lyngby
Denmark

ABSTRACT

In order to evaluate a given ventilation system in a livestock building and its sensitivity to wind, presence of heat sources (e.g. livestock) etc. it is of interest to estimate flow vector fields corresponding to the airflow. By introducing particles (e.g. smoke) into the air inlets of a model of a livestock building, the airflow in a laser-illuminated plane may be visualized. Based on sequences of images recorded of this plane using a video camera, estimates of 2-D flow vectors are derived locally. The local estimates of velocity are found using a set of spatio-temporal convolution filters on the image sequence. After which the local estimates are integrated to smooth flow fields using a model that incorporates spatial smoothness. The algorithms are illustrated using a scale model of a pigs sty under isothermic conditions. It should be noted that this is a non-invasive technique (laser and camera may be placed so they do not disturb the airflow) for estimating air velocity in a 2-D plane.

KEYWORDS

Image Analysis, Optical Flow Estimation, Room Airflow.

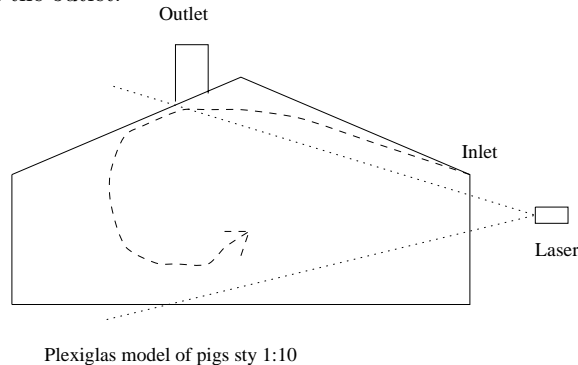
1. INTRODUCTION

At the National Institute of Agricultural Engineering of Denmark air flow patterns in livestock buildings are studied. The purpose being to evaluate the effect of given ventilation systems. In particular it is of interest to determine if draught occurs. Since this may lead to decreasing growth of and increasing sickness among the livestock.

By introducing particles (e.g. smoke) into the air inlets of a model of a livestock building, the airflow in a laser-illuminated plane may be visualized. Based on the recording of a sequence of images (a film) of the patterns occurring in the laser-illuminated plane we may use image analysis to obtain estimates of the optical flow, i.e. the 2-D motion field of the patterns in the illuminated plane.

In the sense that the method described in this article, uses a laser sheet to illuminate particles inserted in the fluid at study, and thus visualizing the flow field, it is similar to the Particle Image Velocimetry reported e.g. in (Westergaard et al. 1993).

FIGURE 1. Experimental setup. The 1:10 plexiglas model of a segment of a pigs sty is illuminated by a laser sheet. The video camera is placed with its optical axis perpendicular to the laser plane. The air is drawn into the model by putting suction on the outlet.



1.1. Estimation of Optical Flow

Independently moving objects, rotation, dilation, and shear in image sequences combine to produce complex velocity fields. Therefore, valid velocity estimation is restricted to local computations. This ensures that for sufficiently smooth velocity fields the velocity can (locally) be assumed translational.

Coherent image translation is the basis for several computational methods. The main methods include correlation-based methods (Wahl and Simpson 1990) of which the Particle Image Velocimetry (PIV) is a special case (Westergaard et al. 1993), differential methods (Horn and Schunk 1981; Nagel and Enkelmann 1986), energy-based methods (Adelson and Bergen 1985; Heeger 1987; Knutsson 1989) and phase-based methods (Fleet 1992).

Restricting measurements to small spatio-temporal neighborhoods, however, often results in the measurements being based on one-dimensional intensity structures (edges and/or lines). In these cases we can only determine the component of the velocity perpendicular to the intensity contour reliably. This is known as the aperture problem.

Because the aperture problem results in flow fields that are not fully constrained an assumption of smoothness of the velocity field must be applied in order to obtain a dense velocity field. One way of doing this is by applying a restriction that force the spatial derivatives to be small. These restrictions are referred to as smoothness constraints. Methods utilizing smoothness constraints include

the work of (Nagel and Enkelmann 1986; Marroquin et al. 1987; Konrad and Dubois 1992).

2. DATA

All data are recorded at the National Institute of Agricultural Engineering of Denmark using a light sensitive consumer video camera (frame rate: 25 Hz). All measurements are carried out under iso-thermic conditions. The experimental setup is shown in Figure 1. The plexiglas model of the segment of a pigs sty is 1 m broad and 0.5 m deep. The air velocity in the inlet is measured to 3 m/s. Smoke is induced in the airflow at the inlet. The laser illuminated plane is placed in the center of the model.

3. METHODS

3.1. Local Estimates of Velocity

Because motion estimation in image sequences can be viewed as identification of patterns repeating themselves over time, it is natural to try to describe the motion analysis in the Fourier domain. Let us consider a neighbourhood containing a one dimensional intensity structure (e.g., a line) that translates coherently through time. In the spatio-temporal domain this corresponds to a neighbourhood of iso-grey level planes. Let these planes be given by their unit normal vector $\hat{\mathbf{k}} = (k_1, k_2, k_3)^T$. We will refer to this vector as the spatio-temporal orientation vector. The non-zero Fourier coefficients of this neighbourhood are

concentrated to the line defined by \mathbf{k} . The correspondence of this vector and the normal flow (i.e. the flow perpendicular to the line) is given by

$$\boldsymbol{\mu} = (\mu, \nu)^T = \frac{-k_3}{k_1^2 + k_2^2} (k_1, k_2)^T \quad (1)$$

Now, in order to estimate this line, we will sample the Fourier domain using a set of spatio-temporal Gabor filters (Gabor 1946) tuned to frequencies distributed evenly across all spatio-temporal orientations, i.e. the center frequencies of the filters are the vertices of a diametrical symmetric regular polyhedron (Knutsson 1989). The p th Gabor filter consists of a Gaussian function shifted to the point $\mathbf{k}_p = (k_{p1}, k_{p2}, k_{p3})^T$ in frequency space. By dividing the filter into an odd and an even part we get the following convolution masks

$$q_p^e(\mathbf{z}) = \frac{\cos(\mathbf{k}_p^T \mathbf{z})}{(2\pi)^{3/2} \sigma^3} \exp\left(-\frac{\mathbf{z}^2}{2\sigma^2}\right) \quad (2)$$

$$q_p^o(\mathbf{z}) = \frac{\sin(\mathbf{k}_p^T \mathbf{z})}{(2\pi)^{3/2} \sigma^3} \exp\left(-\frac{\mathbf{z}^2}{2\sigma^2}\right) \quad (3)$$

Finally, the energy distribution of the Fourier domain as estimated by the set of quadrature filter pairs may be represented by the tensor $\mathbf{T} = \sum_p q_p \mathbf{n}_p \mathbf{n}_p^T$ where q_p is the output from the p th quadrature filter pair, and \mathbf{n}_p is the unit normal vector defining the direction of the filter.

In order to find the direction of maximum spectral density we must find the unit vector \mathbf{k} that maximizes $\mathbf{k}^T \mathbf{T} \mathbf{k}$. This vector is the eigenvector corresponding to the largest eigenvalue of \mathbf{T} . So for the coherently translating one-dimensional intensity structure, which has an effectively one dimensional Fourier domain, the spatio-temporal orientation vector is found by an eigen analysis of \mathbf{T} . Because the Fourier domain is one dimensional \mathbf{T} has only one non-zero eigenvalue.

Now, if the translating structure has a two-dimensional intensity structure (e.g., a grey level corner) the spatio-temporal domain is described by two spatio-temporal orientations, giving rise to two non-zero eigenvalues of \mathbf{T} . The eigenvectors corresponding to these non-zero eigenvalues each translates into a normal flow by using Equation (1). These two normal flows each constrain the true flow in one direction.

We can furthermore determine the perpendicular distance of the true flow to either of the constraint lines, this is given by

$$d_k(x_i, y_i) = \frac{\|(\mathbf{u}(x_i, y_i) - \boldsymbol{\mu}_k(x_i, y_i))^T \cdot \frac{\boldsymbol{\mu}_k(x_i, y_i)}{\|\boldsymbol{\mu}_k(x_i, y_i)\|}\|}{\|\boldsymbol{\mu}_k(x_i, y_i)\|} \quad (4)$$

where $k = 1, 2$, and $\mathbf{u}(x_i, y_i)$, and $\boldsymbol{\mu}_k(x_i, y_i)$ are the true flow and the normal flows taken at the position (x_i, y_i) .

It is the (weighted) sum of squares of these distances that should be minimized across the image in order to obtain the velocity field.

3.2. Integration of Local Estimates of Velocity

Now we will apply an assumption of smoothness with the purpose of fully constraining the velocity field. We do this by forcing the spatial derivatives of the velocity field to be small. One way of formulating such a smoothness constraint is by use of Markovian random fields (Geman and Geman 1984; Konrad and Dubois 1992). We do this using the Bayesian paradigm. First we will formulate a prior distribution for the velocity field based on the spatial derivatives of the field.

Letting the flow at position (x_i, y_i) be given by $\mathbf{u}(x_i, y_i) = (u(x_i, y_i), v(x_i, y_i))^T$ and the corresponding spatial derivatives be denoted by $\mathbf{u}_x(x_i, y_i) = (u_x(x_i, y_i), v_x(x_i, y_i))^T$ and $\mathbf{u}_y(x_i, y_i) = (u_y(x_i, y_i), v_y(x_i, y_i))^T$, the prior distribution of the flow field may be described by a Gibbs distribution $p(\{\mathbf{u}\}) = \frac{1}{Z} \exp(-\beta U_1)$, where Z is a normalization constant and the energy term is given by

$$U_1 = \sum_{i=1}^N [\|\mathbf{u}_x(x_i, y_i)\|^2 + \|\mathbf{u}_y(x_i, y_i)\|^2] \quad (5)$$

where $\|\cdot\|$ is the Euclidean norm. This probability distribution assigns high probability to fields that exhibit small derivatives and low probability to field with high spatial derivatives.

Having constructed this prior distribution for the flow field we will now concern ourselves with an observation model. The observation model relates the local observations or measurements of velocity to any particular realization of the prior distribution.

FIGURE 2. Sub-sequence number 1 shown rowwise, and the estimated flow field corresponding to the center image.

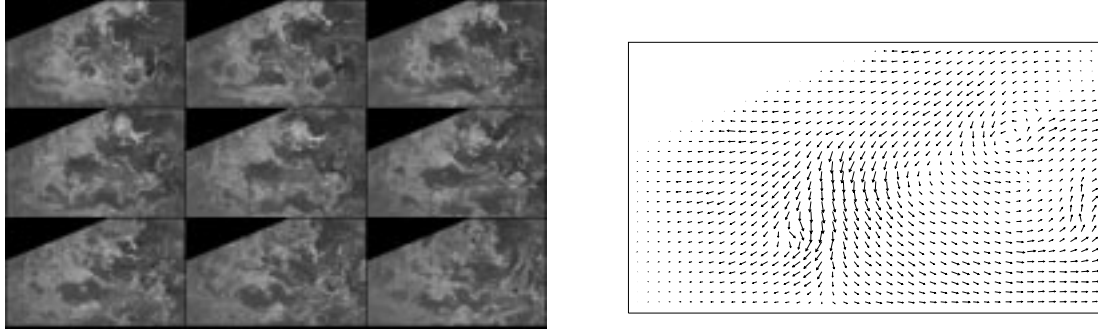
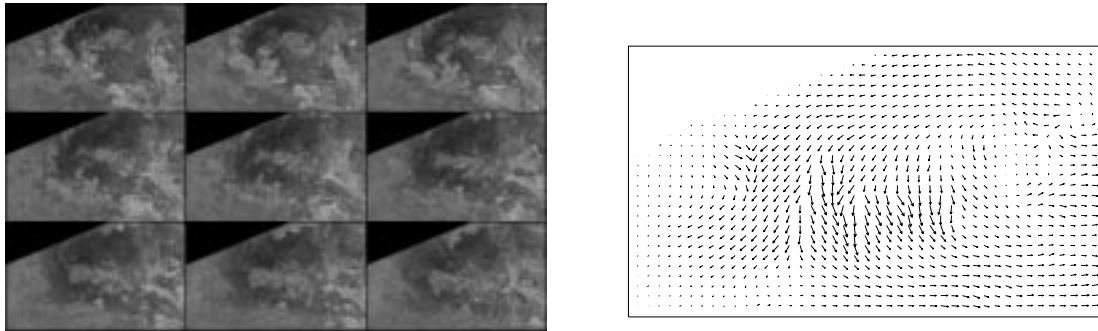


FIGURE 3. Sub-sequence number 2 shown rowwise, and the estimated flow field corresponding to the center image.



$$P(\text{Obs}|\mathbf{u}) = \frac{1}{Z} \exp(-\alpha U_0) = \quad (6)$$

$$\frac{1}{Z} \exp\left(-\alpha \sum_{i=1}^N \sum_{k=1}^2 w_k(x_i, y_i) d_k(x_i, y_i)^2\right)$$

where $d_k(x_i, y_i)$ is the difference between the projection of the true flow onto the normal flow given by the k th eigenvector and the normal flow itself at pixel (x_i, y_i) as described by Equation (5). $w_k(x_i, y_i)$ is an (optional) certainty measure corresponding to this normal flow. Z is a normalization constant. By using a Gibbs energy function that punishes larger deviation in the projection of the true flow onto the observed normal flows we allow smoothing in the direction not constrained by the normal flows while smoothing in the direction of the normal flow is punished.

The prior distribution and the observation model are combined into a posterior distribution using Bayes' theorem. The energy function of the posterior distribution thus becomes

$$U = \alpha \sum_{i=1}^N \sum_{k=1}^2 w_k(x_i, y_i) d_k(x_i, y_i)^2 + \quad (7)$$

$$\beta \sum_{i=1}^N [\|\mathbf{u}_x(x_i, y_i)\|^2 + \|\mathbf{u}_y(x_i, y_i)\|^2]$$

In this energy function we can control the properties of the estimated motion field. The faith in the observed or measured normal flows is controlled by α , the smoothness is controlled by β .

We can now apply a maximization scheme to the posterior distribution in order to obtain the maximum a posteriori estimate of the velocity field.

4. RESULTS

From a video film of the left side of the livestock building model two sub-sequences are extracted. Every other image in these are shown in Figures 2 and 3. The images have 106 rows by 173 columns. The Gabor filters used have a spatio-temporal center frequency of 1.23/pixel and a standard deviation of the Gaussian envelope of 3 pixels.

The estimated flow fields corresponding to the center image in two sequences is shown on the left in Figures 2 and 3. We see that at least qualitatively the flow fields of the sequences are found.

5. DISCUSSION

The method described here should be applicable for flow field estimation in all kinds of fluids.

The derived quantities of the airflow may be used in themselves. Another important application, which we intend to examine, is the use of this method to produce border conditions for Computer Fluid Dynamics computations of the airflow.

It is evident that this algorithm is dependent on particles being visible in the airflow. If the flow is not visualized it can not be estimated.

With respect to the choice of smoothness constraint, the one used here is a simple one, that only requires small first order spatial derivatives of the flow field. It should be possible to use more elaborate models, i.e. models inspired by the physical laws governing the observed phenomena.

The method (as described here) is restricted to 2-D flow fields. But the algorithm can be generalized to the estimation of 3-D flow vectors in space. Experimentally this would require multiplexing the laserplanes, i.e. scanning a volume in planes by moving the laserplane across the volume.

6. CONCLUSION

We have illustrated that based on image sequences of induced particles in airflow illuminated by a laser plane image analysis may be used to estimate the corresponding 2-D flow field. Based on local estimates of motion a model that punishes large first order spatial derivatives is used to find a densely sampled flow field

This technique is noninvasive in the sense that camera and laser can be placed outside the air stream.

7. ACKNOWLEDGEMENTS

The work described in this article was financed by the Danish Agricultural and Veterinary Research Council.

The author is indebted to senior scientists Jan Strøm and Svend Morsing, and technician Peter Ravn of the National Institute of Agricultural Engineering of Denmark for providing image data from the experimental setup at the Airphysics Laboratory at their institution.

REFERENCES

- Adelson, E. H. and Bergen, J. R. (1985). Spatiotemporal energy models for the perception of motion. *Journal of the Optical Society of America, Series A*, **2**(2), 284–299.
- Fleet, D. J. (1992). *Measurement of Image Velocity*. Kluwer Academic Publishers, Norwell, Mass. 203 pp.
- Gabor, D. (1946). Theory of communication. *Journal of the Institution of Electrical Engineers*, **93**, 429–457.
- Geman, S. and Geman, D. (1984). Stochastic relaxation, Gibbs distributions and the Bayesian restoration of images. *IEEE Transactions on Pattern Analysis and Machine Intelligence*, **6**(6), 721–741.
- Heeger, D. J. (1987). Optical flow from spatiotemporal filters. In *First International Conference on Computer Vision*, pp. 181–190 London.
- Horn, B. K. P. and Schunk, B. G. (1981). Determining optical flow. *Artificial Intelligence*, **17**, 185–203.
- Knutsson, H. (1989). Representing local structure using tensors. In Pietikäinen, M. and Rönning, J. (Eds.), *The 6th Scandinavian Conference on Image Analysis*, pp. 244–251 Oulu, Finland. The Pattern Recognition Society of Finland.
- Konrad, J. and Dubois, E. (1992). Bayesian estimation of motion vector fields. *IEEE Transactions on Pattern Analysis and Machine Intelligence*, **14**(9), 910–927.
- Marroquin, J., Mitter, S., and Poggio, T. (1987). Probabilistic solution of ill-posed problems in computational vision. *Journal of the American Statistical Association*, **82**, 76–89.
- Nagel, H.-H. and Enkelmann, W. (1986). An investigation of smoothness constraints for the estimation of displacement vector fields from image sequences. *IEEE Transactions on Pattern Analysis and Machine Intelligence*, **8**(5), 565–593.
- Wahl, D. D. and Simpson, J. J. (1990). Physical processes affecting the objective determination of near-surface velocity from satellite data. *Journal of Geophysical Research*, **95**, 13511–16528.
- Westergaard, C. H., Kock, C. W., Larsen, P. S., and Buchhave, P. (1993). Application of PIV to turbulence studies, - and exploratory study. Tech. rep. AFM-9307, Department of Fluid Mechanics, Technical University of Denmark, Lyngby, Denmark. 49 pp.